

Abstract. At some point in the late-AGB stage, a process (or processes) becomes operative that accelerates and imposes bipolarity upon the slow, spherical AGB winds. What produces bipolarity in these objects and at what stage does bipolarity manifest itself are key questions that remain yet poorly understood.

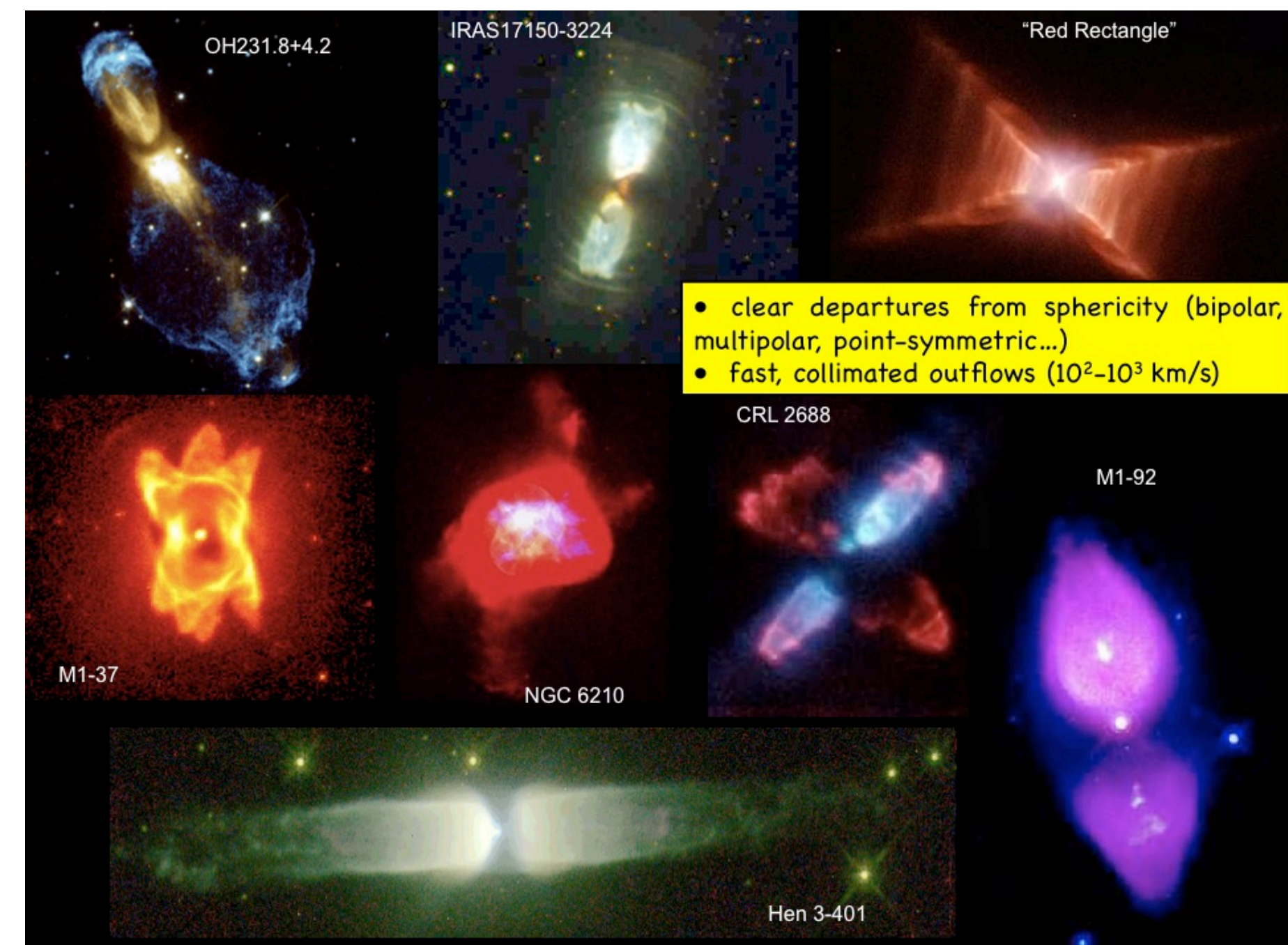
We present CO (115 & 230GHz) mapping of IRAS19374+2359, **an extreme pre-PN with an unparalleled massive, fast molecular outflow** discovered in our OVRO Post-AGB CO 1-0 emission Survey (referred to as OPACOS, Sánchez Contreras & Sahai, submitted to ApJ). We present sub-arcsecond resolution $^{12,13}\text{CO}$ 2-1 and 1.3mm-continuum emission maps recently obtained with the Submillimeter Array (SMA) together with our discovery $\sim 8''$ -resolution $^{12,13}\text{CO}$ 1-0 OVRO maps. The prominent 300 km/s-broad wings and the lack of an intense, low-velocity CO line core in IRAS19374 indicate that most or all of the molecular gas participates in the high-velocity flow. From our CO data, we estimate a total mass in the molecular outflow of $\sim 1 M_{\odot}$ and an unprecedentedly large value for the linear momentum carried of $\geq 45 M_{\odot}\text{km/s}$. Our SMA maps show CO emission arising from a $\sim 3'' \times 2''$ hourglass-shaped molecular flow aligned with the optical lobes; a linear velocity gradient along the lobes as well as equatorial expansion at the nebula waist are found. The spatio-kinematic structure of this object is in support of a jet-envelope entrainment scenario in which a substantial amount of directed momentum is transferred to large parts of the dense AGB wind by interaction with fast, collimated post-AGB jets.

1. INTRODUCTION

PPNs & PNs evolve from envelopes around AGB stars

Biggest challenge: understanding PPNe shaping!

- AGB circumstellar envelopes (CSEs): spherical symmetry & expand slowly (10-20 km/s)
- PPNe/PNe, however... (aspherical & fast flows – 10^2 - 10^3 km/s) (Balick & Frank 2002 for a review)



• PPNe/PNe, however... Momentum excess problem (Bujarrabal et al. 2001): $P > L/c \times t_{\text{pAGB}} \rightarrow$ Post-AGB mass loss NOT driven by pulsation+radiation pressure on dust (unlike AGB mass loss).

Post-AGB shaping: Interacting winds? (Sahai & Trauger 1998)

Interaction between:
fast, collimated (jet-like) winds +
pre-existing AGB CSE (spherical and slow)
 \rightarrow shocks shape and accelerate AGB CSE.

- ✓ Jet launching & collimation mechanism? (binaries? MHD?)
- ✓ When do jets appear for the first time? ($\sim M_{\text{loss stop}}$)
- ✓ What triggers their appearance? (intrinsic vs. extrinsic factors?)
- ✓ etc ... UNKNOWN!!

Characterization of post-AGB CSEs: components, morphology, dynamics... IS NEEDED

Post-AGB CSEs are cold ($\sim 20\text{K}$) – bulk of the mass is MOLECULAR \rightarrow CO best tracer of molecular gas, easy to interpret (thermalized in most nebular regions) \rightarrow density, temperature & velocity distribution.

CO mm-wave observations probe mass-loss history and circumstellar evolution (nebular shaping/acceleration by wind interaction) on the AGB and beyond (post-AGB)

2. IRAS 19374+2359

First suggested to be a PPN candidate by Kwok et al. (1987):

- OH/IR star
- low IRAS color temperature ($\sim 200\text{K}$)
- lack of variability
- Optical counterpart
- \rightarrow Detached dust envelope (AGB M_{loss} stopped)

- Remains poorly studied
- Optical HST image: $3'' \times 2''$ bipolar nebula + scattering halo (Fig. 4)
- $\text{H}\alpha$ emission with ~ 600 km/s-broad wings from the stellar vicinity: on-going fast pAGB ejection (Sánchez Contreras et al. 2008).
- central star: B3-6 I (Sánchez Contreras et al. 2008).
- $9.7\mu\text{m}$ silicate absorption feature \rightarrow O-rich (Lawrence et al. 1990)
- H_2 line emission from shocked molecular gas (Kelly et al. 2005).
- The distance is estimated to be 11 kpc, $\rightarrow L \sim 9 \times 10^4 L_{\odot}$ (SCS12).
- No previous CO detection (Hu et al. 1994)

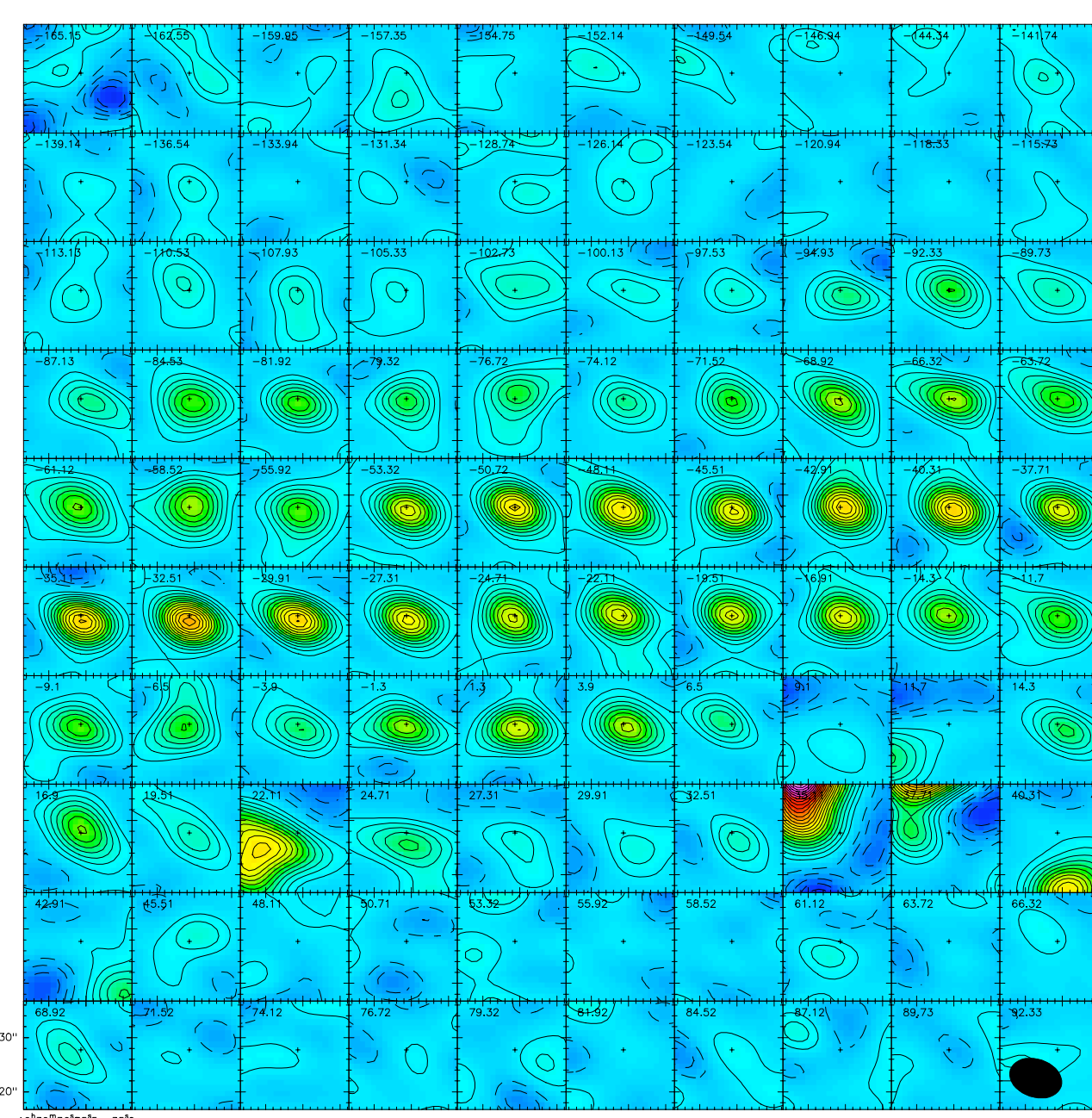


Fig. 1: Our discovery OVRO ^{12}CO 1-0 maps of IRAS 19374: a) Velocity-channel maps (box-marking V_{LSR}). The emitting source is unresolved in these $\sim 8''$ -resolution maps.

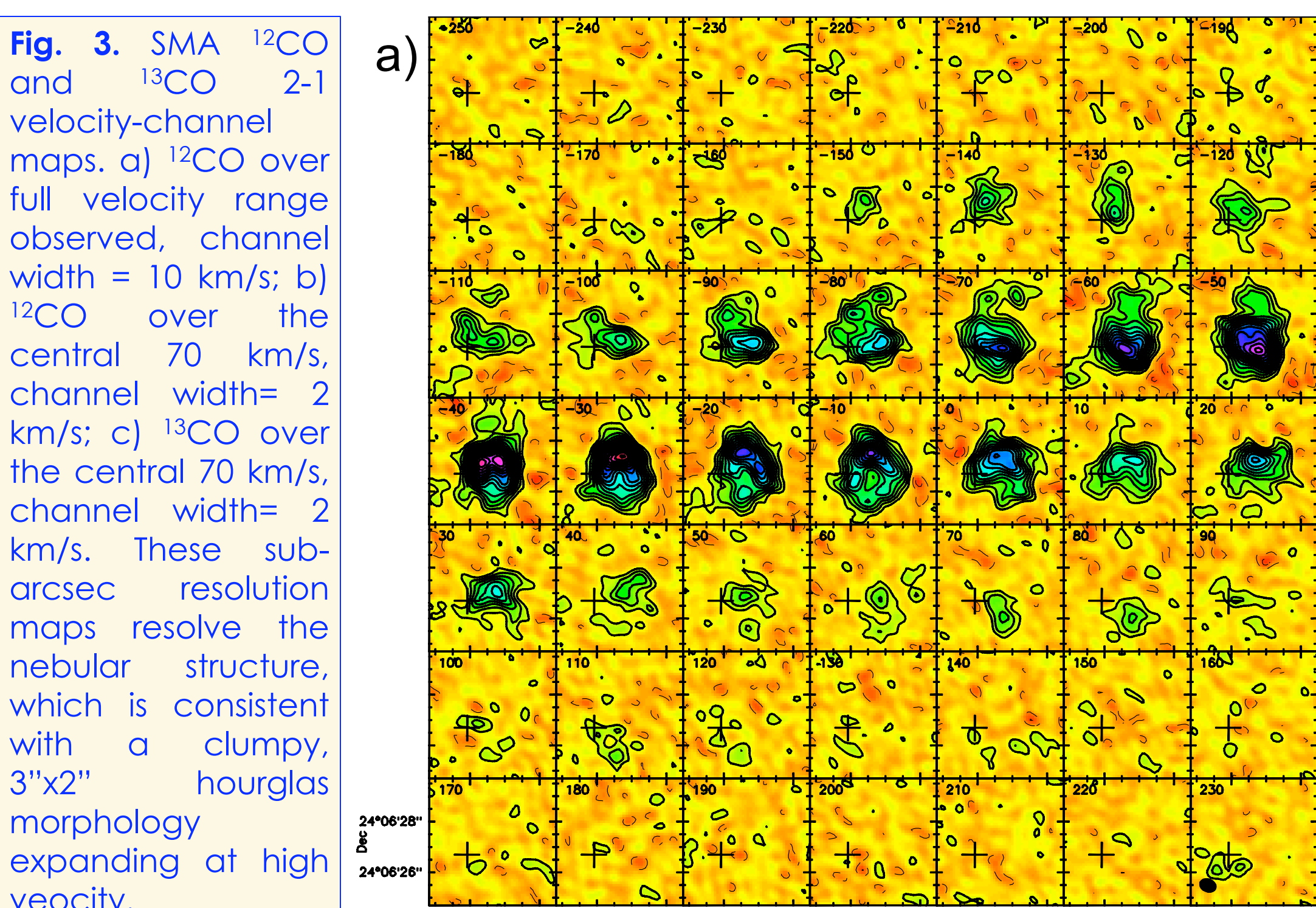


Fig. 3. SMA ^{12}CO and ^{13}CO 2-1 velocity-channel maps. a) ^{12}CO over full velocity range observed, channel width = 10 km/s; b) ^{12}CO over the central 70 km/s, channel width = 2 km/s; c) ^{13}CO over the central 70 km/s, channel width = 2 km/s. These sub-arcsec resolution maps resolve the nebular structure, which is consistent with a clumpy, $3'' \times 2''$ hourglass morphology expanding at high velocity.

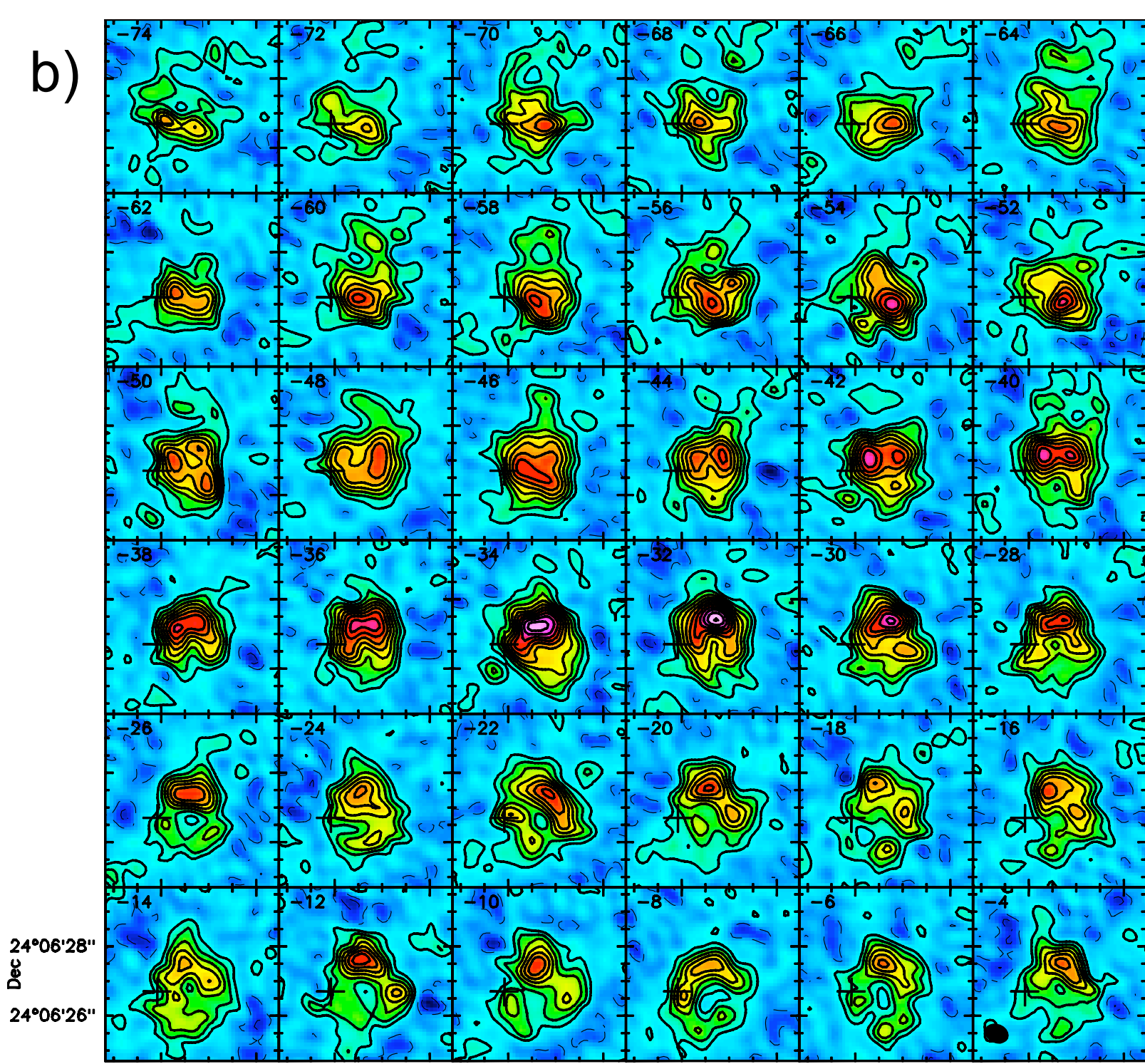


Fig. 4. SMA ^{12}CO and ^{13}CO 2-1 position-velocity diagrams along the symmetry axis of the nebula (roughly oriented along the NS direction, i.e. Dec. axis) and in the perpendicular direction (R.A.). Note the linear velocity gradient and large (projected) expansion velocities reached (up to ~ 150 km/s)

3. Observations and Main Results

We detected ^{12}CO and ^{13}CO 1-0 emission in IRAS19374 for the first time in our OPACOS CO survey of post-AGB objects (Sánchez Contreras & Sahai, submitted to ApJS; SC&S12). We have performed follow up observations with SMA and IRAM 30m (see Tables 1 and 2).

Table 1. Observing Log

Facility	Date	Configuration	HPBW	PA	Observations
OVRO	May-2003 Sep-2003	C	$9''.8 \times 7''.0$	72°	^{12}CO ($J=1-0$), ^{13}CO ($J=1-0$), 2.6mm-continuum
SMA	Jul-2009, Sep-2010, Sep-2011	EX, VEX	$0''.7 \times 0''.5$	67°	^{12}CO ($J=2-1$), ^{13}CO ($J=2-1$), 1.3mm-continuum
IRAM 30m MRT	Jun-2007	-	$\sim 10''.7$	-	^{12}CO ($J=2-1$)

Table 2. Line parameters

Transition	Rest Freq. (GHz)	V_{LSR} (km/s)	FWHM (km/s)	FWZI (km/s)	Ipeak [$1\sigma^*$] (Jy/beam)	Flux [1σ] (Jy*km/s)
^{12}CO ($J=2-1$) ^a	230.5380000	-37 ± 3	86 ± 5	300	0.39 [0.03]	190 [10]
^{12}CO ($J=2-1$) ^b	"	-33 ± 2	125 ± 5	300	1.36 [0.14]	182 [5]
^{13}CO ($J=2-1$) ^a	220.3986842	-33 ± 3	50 ± 3	150	0.16 [0.02]	27 [1]
^{12}CO ($J=1-0$) ^c	115.2712018	-37 ± 2	95 ± 3	160	0.54 [0.04]	39 [2]
^{13}CO ($J=1-0$) ^c	110.2013543	-31 ± 4	~ 10	~ 15	~ 0.12 [0.03]	4.5 [1.2]

a: SMA; b: IRAM 30m MRT ($S/T_{\text{A}}^* = 8$ Jy/K @ 230GHz); c: OVRO
* Spectral resolution $\Delta v \sim 2.6$ km/s

Our OPACOS data revealed a broad CO emission line with a remarkable triangular shape (Figs. 1 & 2). This wing-dominated profile differs from those seen in most pPNe, with an intense line core at low velocity and, in some cases, weak broad wings. The CO 2-1 single-dish spectrum shows a similar wing-dominated profile with an even larger full velocity extent (FWZI ~ 300 km/s). The CO envelope is unresolved in our OPACOS maps (HPBW $\sim 9''.8 \times 7''.1$).

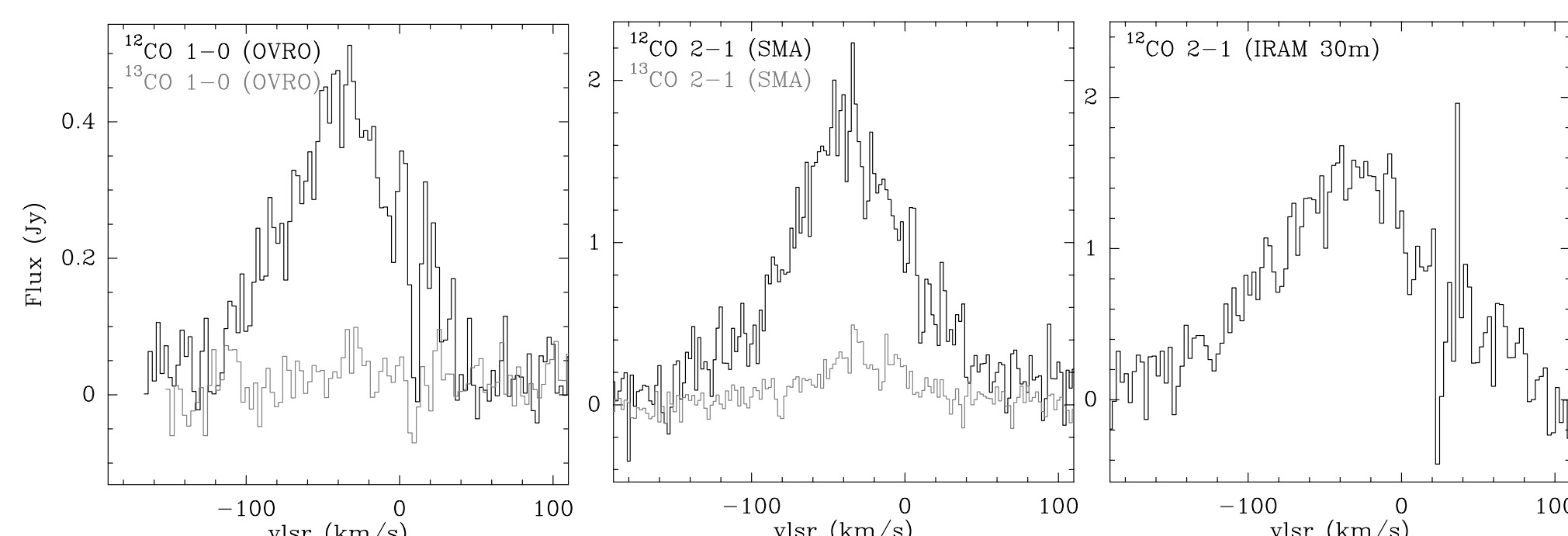


Fig. 2. OVRO, SMA, and IRAM-30m integrated CO line profiles. The broad wings indicate that most of the molecular gas participates in the high velocity outflow.

Our sub-arcsec resolution CO maps at 230 GHz with the SMA (Figs. 3-5) show emission over a ~ 300 km/s velocity range arising from a $3'' \times 2''$ bipolar molecular flow very well aligned with the optical nebula. The p-v diagrams suggest an overall, yet rather clumpy, hourglass morphology, with polar outflows and a dense toroidal structure expanding orthogonally to the lobes. This type of morphology is observed in other PPNs, e.g. M2-56 and He3-1475 (Castro-Carrizo et al. 2002, Huggins et al. 2004). Our maps suggest that the lobes of IRAS19374 may be incomplete, shell-like structures (i.e. "hollow") with closed ends. The molecular outflow of IRAS 19374 has a subtle point-symmetry, which is also hinted in the optical HST and that could point to an underlying precessing bipolar wind.

Both molecular components, i.e. the lobes and the torus, are characterized by a linear velocity gradient (so-called Hubble-type outflow) of 100 and $35 \text{ km s}^{-1} \text{ arcsec}^{-1}$, respectively. The (projected) expansion velocity increases from $V_{\text{exp}} - V_{\text{sys}} \sim 20$ km/s, near the center, up to $V_{\text{exp}} - V_{\text{sys}} \sim 150$ km/s at the tip of the South lobe. In the central, equatorial region the (projected) expansion velocity reaches a maximum value of $V_{\text{exp}} - V_{\text{sys}} \sim 20$ km/s.

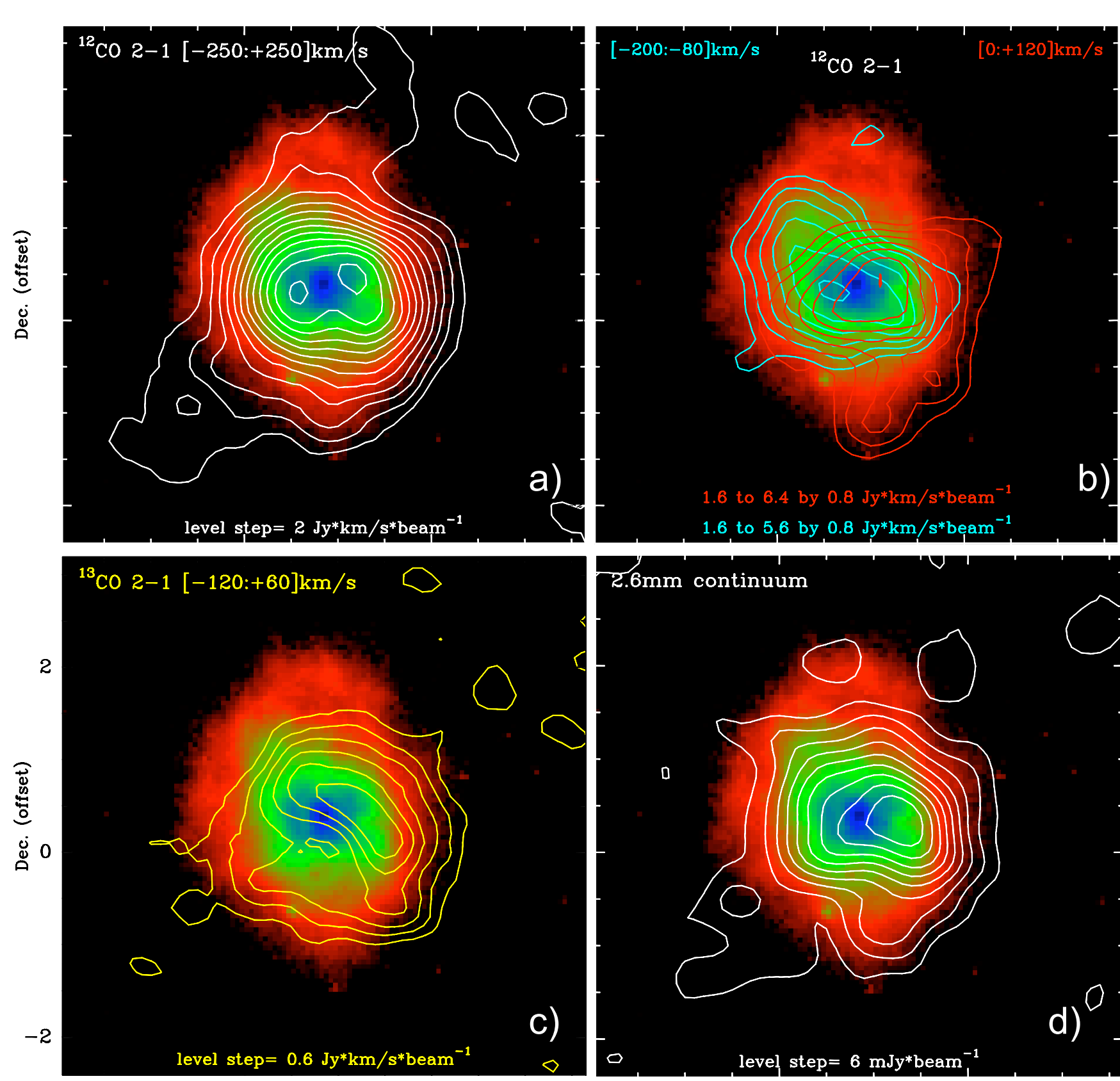


Fig. 5. SMA maps (contours) overlaid on a false-color HST image of IRAS19374: a) velocity-integrated ^{12}CO 2-1 maps; b) ^{12}CO 2-1 emission integrated over the red and blue emission wings; c) velocity-integrated ^{13}CO 2-1 maps; d) 1.3 mm continuum map.

The Hubble-type outflow (Fig. 4) suggests constant-velocity, ballistic motions resulting from a sudden interaction between a bipolar post-AGB wind and the AGB CSE (Alcolea et al. 2001). The radial expansion observed indicates a kinematical age for the outflow and the equatorial structure of ~ 650 - $950 \tan(i)$ yr and $\sim 1500/\tan(i)$ yr, respectively, with i being the inclination of the polar axis with respect to the plane of the sky. Adopting a moderately low value of $i \approx 30^\circ$, suggested by the similar colors and surface brightness of the optical lobes, the dynamical age of the lobes ~ 500 yr, whereas the age of the central torus would be ~ 2600 yr.

Our ^{13}CO 2-1 SMA maps confirms the presence of the dense torus, however, there are notable differences in the detailed structure of the low velocity component as revealed by the ^{13}CO and ^{12}CO 2-1 transitions (Figs. 3 & 4), indicating that ^{13}CO ($J=2-1$), due to its lower optical depth, is a better probe of the inner nebular regions.

Continuum emission at 1.3mm is detected from a central $\sim 2''$ -sized region with a similar hourglass-distribution. The total 1.3mm flux integrated over the source is ~ 35 mJy and is consistent with cold dust emission (Fig. 6)

Table 3. Physical parameters derived from preliminary analysis

M_{gas} (M_{\odot})	M_{dust} (M_{\odot})	P_{min} (M_{\odot})	X_{AGB} (%)	$^{12}\text{C}/^{13}\text{C}$	R_{lobes} (cm)	R_{torus} (cm)	t_{lobes} (yr)	t_{torus} (yr)	M_{loss} (M_{\odot})
1.0	0.03	47	80	~ 9	2.4×10^{17}	7×10^{16}	~ 500	~ 2500	2×10^{-5} - 2×10^{-4}

$X(^{13}\text{CO-to-H}_2) = 2 \times 10^{-5}$, $T_{\text{ex}} = 5$ - 20K , $d = 11$ kpc
Dust grains $a \sim 1\mu\text{m}$, $\rho = 3 \text{ gr cm}^{-3}$

Final remarks. The prominent wings and the lack of an intense, low-velocity line core in IRAS 19374 indicate that most or all of the molecular gas participates in the high-velocity flow. We estimate a total mass in the outflow of $\sim 1 M_{\odot}$ (from the optically thin ^{13}CO 1-0 transition) and an unprecedentedly large value for the linear momentum carried by the outflow of $> 45 M_{\odot}\text{km/s}$. To the best of our knowledge, there are only two other pPNe displaying similar wing dominated CO profiles, He3-1475 and IRAS 22036, although the mass and momentum of their fast outflows are much smaller than in IRAS19374. Our maps of IRAS19374 support the jet-envelope entrainment scenario since the CO wings are found to arise in bipolar structures and, therefore, it is likely that most of the molecular gas in the massive, slow AGB wind of IRAS 19374 has been affected by the shock interaction with fast, post-AGB jets. However, the origin of such large momentum and the launching mechanism remain to be understood.

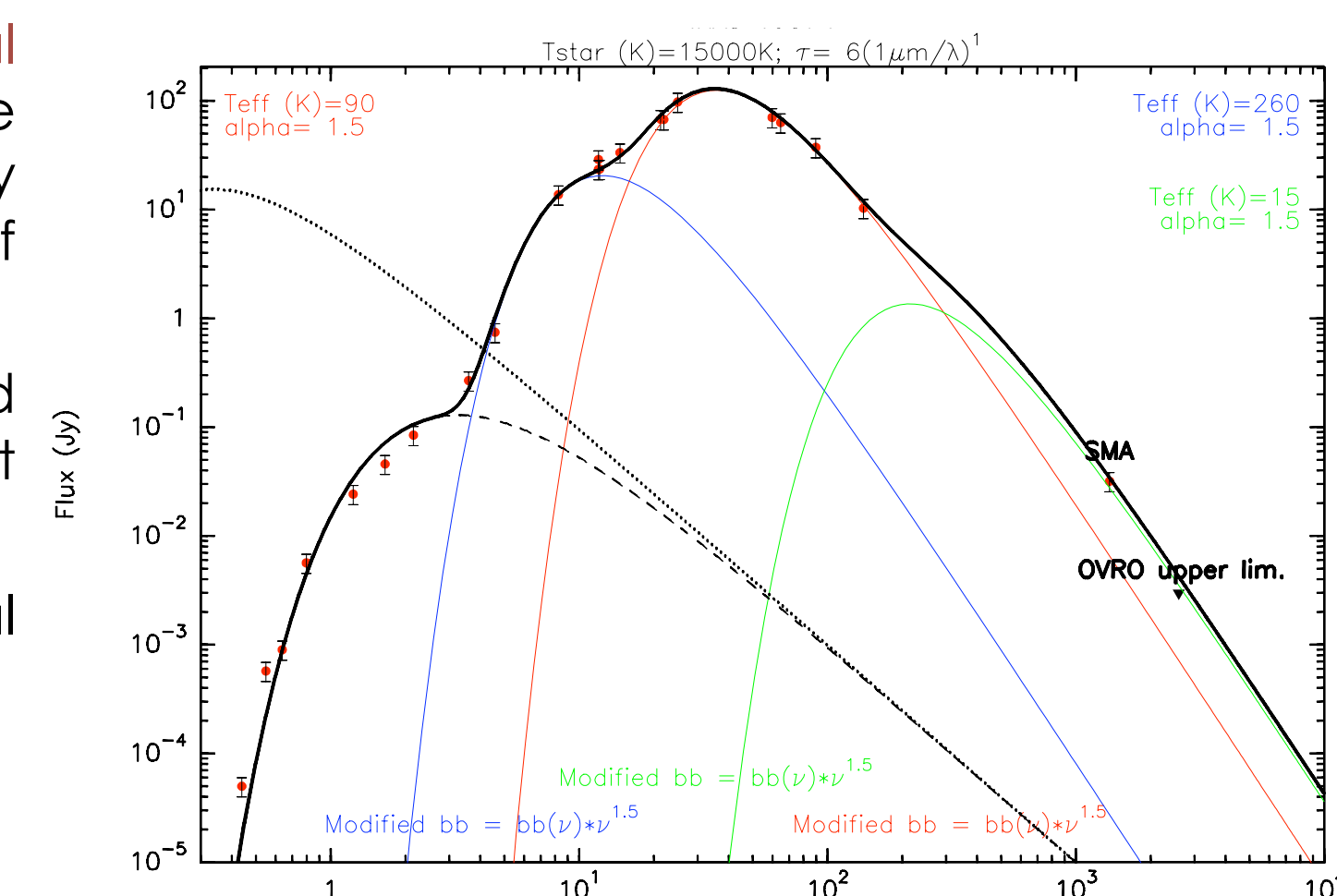


Fig. 6. Spectral energy distribution (SED) of IRAS 19374. Red circles represent GSC2, 2MASS, WISE, MSX, AKARI, IRAS, and SMA data points; our OVRO upper limit to the 2.6mm continuum flux is represented with a triangle. The SED has been fitted by a very simple, preliminary model for the dust emission using 3 different components (with mean temperatures of 260, 90, and 15K) and assuming that the grains emit as modified black-bodies with a spectral slope $\alpha \sim 1.5$. The stellar spectrum, with and without dust extinction, is also fitted (dotted and dashed lines, respectively).